Colloidal submicron-palladium particles stabilized with acetate

Koichi. Aoki*, Yanhong Zhao, Jingyuan Chen

Department of Applied Physics, University of Fukui, 3-9-1Bunkyo, Fukui-shi, 910-8507 Japan

Abstract

Palladium spherical particles 0.23 μm in diameter were synthesized by reducing palladium acetate with hydrazine in the presence of surfactant, with an aim of exhibiting both easy separation by filtration and easy dispersion for a catalyst. The particles in the suspension were sedimented slowly but not aggregated. The suspension showed voltammetric redox waves. The anodic wave was ascribed to the oxidation of Pd to Pd^{2+}, whereas the cathodic one was to the reduction of the palladium acetate moiety to Pd. The current ratio of the anodic peak to the cathodic one, 4:1, was close to the ratios by the partial chemical oxidation with permanganate and by the thermogravimetry, suggesting the composition of 80 % palladium metal and 20 % palladium acetate in the molar ratio. Heating the palladium particles at 300 ^{o}C yielded palladium metal. The decomposition proceeded to the first-order reaction with the activation energy of 40 kJ mol^{-1}. The particle catalyzed the reduction of methylene blue with hydrazine. The reaction rate was of the first-order with respect to methylene blue. The rate constant was proportional to the geometrical surface area of the palladium particle, suggesting a surface catalysis.

Key words: palladium particles, voltammetry, submicron, catalysis, thermogravimetry

* e-mail d930099@icpc00.icpc.fukui-u.ac.jp (K. Aoki)

Introduction

Colloidal suspensions of big particles such as polymer microspheres and metal particles are sustained against aggregation with stabilizers which cover the surface of colloidal particles [1]. The stabilizers often used are surfactants and monolayer films such as alkylthiolates [2-5], carboxylates [6,7], thioether [8], amino acids [9], and isocyanide [10]. The stabilizers for colloidal suspensions are chemically bonded onto the central material, and hence are different from adsorbed surfactants in micelles or emulsions [11]. The colloidal particles are composed of at least two compounds, a surface layer called a shell and a central material called a core. An example of the well-examined core-shell structure is the thermally synthesized silver stearate nanoparticles [12-15], which is composed of 9.4 % molar ratio of the shell of silver stearate and 90.6 % of the core of silver atom [16]. It is important to identify and to determine quantitatively the two compounds in order to evaluate their reactivity and specify the structure. However, work in this direction is limited [16,17], probably because more interest has been taken in exploiting functionality.

The smaller are the particles, the more stable is the dispersion in solution and the higher is the chemical activity. However, it is more difficult to separate and purify smaller particles, as is exemplified by redox active latex particles [18-20]. Metal nanoparticles have not been purified enough to exhibit well-defined voltammograms [7,21]. On the contrary, large particles readily sedimented with centrifugation can be purified sufficiently to remove salts from the suspension until showing iridescence [22,23]. Furthermore, their surface has been modified by conventional film techniques [18-20,24] and a layer-by-layer method [25-27]. Consequently, larger particles have advantages in chemical modification.

We consider here a quantitative relation between the amount of the shell and the size. It is assumed that a spherical particle in radius r is composed of N core-molecules and that its surface is packed in a monolayer form with n cubic shell-molecules. If the

volume of the single core molecule, a^3, is close to that of the single shell molecule, the volume of the particle is given by $(4\pi/3)r^3 = Na^3$. Since the surface area of the particle is represented by $S = 4\pi r^2 = 4\pi(3Na^3/4\pi)^{2/3}$, the ratio of the number of the shell-molecules, S/a^2, to that of the core-molecules, N, becomes $(S/a^2)/N = (36\pi)^{1/3}N^{-1/3} = 4.8N^{-1/3}$. Numerical values of the number ratio are 0.48, 0.22, 0.10 and 0.05 for $N = 10^3$, 10^4, 10^5 and 10^6 (corresponding to r = 1.6, 3.4, 7.3, 15.8 nm for the density 10 g cm^{-3}), respectively [7]. This calculation has been demonstrated to be nearly valid for the silver stearate nanoparticles for r = 2.5 nm. For palladium nanoparticles often investigated, the diameters range 2 to 8 nm [28-37], which corresponds to N = 500 - 2000 and $(S/a^2)/N$ = 0.6 - 0.18. The non-negligible values of the ratio indicate a significant contribution of shells. In contrast, a submicron particle, e.g., r = 0.1 μm, has the ratio, 0.0056, and hence the amount of the surfactant is as little as impurities. This value seems to be too small for conventional synthetic conditions of the amount of a surfactant. Either case may be realized: only the small amount of stabilizers participates in forming particles; or a particle has no core-shell structure but takes a mixture. Submicron particles may be different from conventional nanoparticles in structure.

Our concern here is directed to the structure as well as the functionality of submicron palladium particles. This report deals with synthesis of submicron palladium particles stabilized with palladium acetate, determination of the number ratio of the stabilizer to the metal, and catalytic efficiency for methylene blue.

Experimental

Chemicals

Palladium acetate (99.9 %, Aldrich), poly-(vinyl pyrrolidone), abbreviated as PVP, with 40,000 molecular weight, hydrazine (98.0 %, Kanto), tetra-n-butylammonium hexafluorophosphate abbreviated as $TBAPF_6$ (TCI), dichloromethane (99.9 %, Wako)

were used as received. Acetonitrile (99.5 %, Wako) was treated with molecular sieves, 4A 1/8 (Wako) before electrochemical measurements. Water was distilled and ion-exchanged.

Palladium particles were synthesized as follows. 100 cm^3 ethanol solution including 20 mg palladium acetate was mixed with 100 cm^3 water containing 80 mg PVP, exhibiting yellow color. 5 mg Hydrazine was added to the mixture that was deaerated by N_2 for 20 min in advance. The mixture was refluxed for 5 h, and re-dispersed in a mixture of water and ethanol (1:1 v/v), water, ethanol, and ethanol in turn. The rinsed material was centrifuged, re-dispersed in water, centrifuged again, and re-dispersed in ethanol. The purified suspension in ethanol was turbid. It was filtrated with microfilter with 0.2 μm pores and then the filtrated solution was black transparent. The product was dried at room temperature and got in powder form.

Electrochemical and other measurements

The Pt and Pd disks 1.6 mm in diameter (BAS) were used as working electrodes. The $Ag|Ag_xO$ was used as a reference electrode, of which potential was more positive by 0.053 V than an Ag|AgCl reference electrode in 3 M NaCl.

UV- and vis-spectrometry was carried out with UV-570 (JASCO). Scanning electron microscopy (SEM) was made with SH-600 (Hitachi) for the Pd particles at 13 kV. The instrument of thermogravimetry was home-made by combining a balance and a thermo-controlled oven through which nitrogen gas flowed.

Results and Discussion

Formation of Pd particles

The mixture of palladium acetate, PVP and hydrazine showed pale yellow color.

The reflux changed the color of the solution into almost transparent black. The UV spectra (Figure 1) show not only consumption of palladium acetate at 400 nm after the reduction but also replacement of the ultraviolet band by the broad visible band [38]. The appearance of the visible band supports formation of an electronic band structure of palladium particles [39,40]. In contrast, the disappearance of the band at 400 nm is due to making the spectrum featureless by light scattering. The reduction of palladium acetate may be obeyed by [41,42]

$$N_2H_4 \cdot H_2O \rightarrow N_2H_5^+ + OH^- \quad (1)$$

$$Pd^{2+} + 2N_2H_5^+ + 10OH^- \rightarrow Pd + 2N_2 + 10H_2O + 6e^- \quad (2)$$

If *k* palladium atoms and *m* palladium acetate molecules form a particle with the help of PVP, the reaction is given by

$$kPd + mPd(CH_3COO)_2 \rightarrow Pd_k\,[Pd(CH_3COO)_2]_m \quad (3)$$

Figure 2 shows the SEM photographs of the palladium particles before (A) and after (B) the centrifugation and the filtration through the 0.2 μm micropore filter. Two sizes of spherical particles 0.2 and 2 μm in diameter are appreciable before the treatment (A). The appearance of the uniform diameter, 0.23±0.04 μm, after the treatment is obviously due to the removal of small particles and residues by the centrifugation and of large particles by the filtration. The size distribution after the treatment is shown in Fig.2(C).

The treated particles did not dissolve in aqueous solutions, acetonitrile or dichloromethane, but were dispersed in a form of a turbid suspension. The suspension in acetonitrile was stable for more than one day without sedimentation or aggregation.

The particles were reduced neither with ferrous ion nor ascorbic acid. In contrast, they were oxidized with MnO_4^- in acidic solution, as was demonstrated by disappearance of the purple color of MnO_4^- immediately after the addition of the particles. Since the oxidized moiety in the particles is palladium metal, the oxidation may occur according to the reaction:

$$Pd + MnO_4^- + 4H^+ + e^- \rightarrow Pd^{2+} + MnO_2 + 2H_2O \quad (4)$$

One palladium particle consumes k MnO_4^- molecules (see Eq.(3) and (4)). We titrated 3.30 mg Pd particles with 0.02 M $KMnO_4$ in 1 M H_2SO_4, and consumed 1 cm^3 $KMnO_4$ solution until the end point. If the Pd particle is composed of only Pd and $Pd(CH_3COO)_2$, as is shown in Eq.(3), its weight per mole is $106.4k + 224.5m$, where 106.4 and 224.5 are molar weights of Pd and $Pd(CH_3COO)_2$, respectively. The result of the titration leads to the equality: $3.3\times10^{-3}k / (106.4k + 224.5m) = 0.02\times10^{-3}$, which yields $m/k = 0.26$. The mass ratio and molar ratio of Pd metal to that of one particle are 64 % and 80 %, respectively.

The above calculation is based on the assumption of only the two components in the particle. However, the particle necessarily includes the surfactant, PVP. Otherwise, it would be aggregated and precipitated. In order to determine the amount of PVP in the particle, we dispersed the particle into water and took the UV spectra. The absorbance at 195 nm, which can be assigned to aqueous solution of PVP, was used for determination of PVP. The weigh ratio and the molar ratio of PVP to the particle are, respectively, 0.033 and 1.1×10^{-4}. Consequently, PVP has a negligible contribution to the evaluation of m/k.

Metal nanoparticles are known to have lower melting points than those of bulk metal. The lower shift of the melting points has been considered to be due to an excess of surface energy of nanoparticles [43-54] or Kelvin's effect [55]. The other concept is thermal removal of the surfactant and aggregation, as has been found for silver fatty acid nanoparticles [16,56]. In order to estimate an apparent melting point, thermogravimetry was applied to the present Pd particles. Vacuum-dried particles were heated at several temperature scan rates in nitrogen atmosphere during which they were weighed. Figure 3 shows the variation of the weight ratio with the temperature. The weight loss began at 210 ^oC and then reached a constant value over 400 ^oC. This variation is similar to the thermal decomposition of silver stearate nanoparticles to silver

metal and organic gas [16,56], and hence the decomposition of the Pd particles may follow

$$Pd_k[Pd(CH_3COO)_2]_m \rightarrow (k + m)Pd + gas \quad (5)$$

20 % Weight loss indicates the equality $0.8\times(106.4k + 224.5m) = 106.4(k + m)$ should hold. Consequently we obtain $m/k = 0.29$, which is close to the value (0.26) obtained from the oxidative titration by $KMnO_4$. The product by heating at 400 ^oC was metal-like solid with bright white color. Palladium becomes metal at 400 ^oC although the melting temperature is 1554 ^oC.

The thermogravimetric curve in Figure 3 was analyzed on the assumption of the first-order decomposition kinetics, according to the concept of the thermal decomposition of silver nanoparticles [16]. Letting the weight ratio in Figure 3 be x, the ratio varies with the temperature in the following way [16]

$$\ln[(-\ln x)T^{-2}] = \ln(AR/uU) - U/RT \quad (6)$$

where U is the activation energy of the first-order decomposition, A is the frequency factor, and u is the temperature scan rate. Plots of $\ln[(-\ln x)T^{-2}]$ versus T^{-1} are shown in Figure 4, falling on a straight line over the domain from 210 to 360 ^oC. The slope should be $-U/R$ and hence we obtain the activation to be 40 kJ mol^{-1}. The large value suggests the significance of reaction (5) rather than simple thermal fusion.

Electrochemistry

Figure 5 shows cyclic voltammograms of Pd particles-suspended acetonitrile solution including 0.05 M tetrabutylammonium hexafluorophosphate ($TBAPF_6$). There were mainly the anodic wave at 1.72 V (a) and the cathodic wave at -0.32 V (b). Appearance of these well-defined waves is ascribed to the purification by iterative centrifugation and re-dispersion. The voltammogram only at the anodic scan starting at 0.5 V was almost the same as the anodic part in Figure 5, and the voltammogram at the cathodic one was similar to the cathodic part. Therefore, there is no redox pair in the

potential domain across 0.5 V. Since the cathodic wave at 1.0 V appeared only when the reverse potential went over 1.9 V, it is due to oxidation products at 2.0 V. Anodic wave (a) can be attributed to the oxidation of Pd of the particle to Pd^{2+} because the palladium electrode showed a rise of the anodic dissolution wave at 1.6 V, as is shown in curve (d) of Figure 5. Values of the peak current were proportional to the concentration of Pd particles. When the suspension was kept quiescent until it got transparent owing to sedimentation, its voltammogram showed no neither anodic nor cathodic wave. These facts confirm the attribution of wave (a) to Pd(in particle) $\rightarrow$ Pd^{2+}.

It is predicted that the cathodic wave is attributed to the reduction of palladium acetate moiety in the particles. As a control experiment for attribution of wave (b), we made voltammetry of the solution of the palladium acetate molecule. The voltammogram had a cathodic wave at -0.55 V, which is ascribed to the reduction

$$Pd(CH_3COO)_2 + 2e^- \rightarrow Pd + 2CH_3COO^- \quad (7)$$

The positive shift of the reduction wave for the Pd particles (at -0.32 V) indicates that the palladium acetate moiety is more unstable by 22 kJ mol^{-1} (= F(0.55-0.32)V) than the palladium acetate molecule. The unstableness is ascribed to a loss of solvation energy owing to packed palladium atoms in the Pd particle.

The anodic peak currents and the cathodic ones were proportional to the concentration of the Pd particles, as is shown in Figure 6. They were also proportional to the square-root of the potential scan rate, as is shown in Figure 7. Consequently, both the peak currents are controlled by diffusion of the particles. The ratios of the anodic slope to the cathodic one are 0.31 and 0.28 for the I_p vs. c and I_p vs. $v^{1/2}$, respectively. The expression for the diffusion-controlled peak curren of the concomitant n-electron transfer reaction is expressed by [57]

$$I_p = 0.446n^{3/2}FAcD^{1/2}v^{1/2}(F/RT)^{1/2} \quad (8)$$

where D is the diffusion coefficient of the particle and A is the area of the electrode. On the other hand, the expression for the consecutive n-electron transfer reaction is

expressed by [58]

$$I_p = 0.446nFAcD^{1/2}v^{1/2}(F/RT)^{1/2} \quad (9)$$

When the two equations are applied to the 2*k*-electron oxidation for the Pd particle, the anodic peak current are expressed, depending on the 2-electron concomitant or the 2-electron consecutive reaction, by

$$(I_p)_{A,com} = 0.446(2k)\sqrt{2}FAcD^{1/2}v^{1/2}(F/RT)^{1/2} \quad \text{(concomitant)} \quad (10A)$$

$$(I_p)_{A,sec} = 0.446(2k)FAcD^{1/2}v^{1/2}(F/RT)^{1/2} \quad \text{(consecutive)} \quad (10B)$$

The cathodic peak currents are similarly give by

$$(I_p)_{C,com} = -0.446(2m)\sqrt{2}FAcD^{1/2}v^{1/2}(F/RT)^{1/2} \quad \text{(concomitant)} \quad (11A)$$

$$(I_p)_{C,sec} = -0.446(2m)FAcD^{1/2}v^{1/2}(F/RT)^{1/2} \quad \text{(consecutive)} \quad (11B)$$

There are four combinations of the ratios of the cathodic current to the anodic current, e.g., $(I_p)_{C,com}/(I_p)_{A,sec}$. Since variables of *F*, *A*, *c*, *D* and *v* are common to the four equations, the ratios are reduced to m/k, $m/2^{1/2}k$ and $2^{1/2}m/k$, as is shown in Table 1. Equating these variables to the experimental values of the $(I_p)_C/(I_p)_A$ obtained from the relations of I_p vs. *c* (Figure 6) and I_p vs. $v^{1/2}$ (Figure 7), we determined values of m/k for the four cases. It is the value 0.28 in Table 1 that is close to 0.26 - 0.29 obtained for the titration and the thermogravimetry. This case corresponds to $(I_p)_{C,com}/(I_p)_{A,com}$ and $(I_p)_{C,sec}/(I_p)_{A,sec}$. Both the anodic and the cathodic 2-electron reactions are either concomitant or consecutive, although we cannot assign the either electron transfer step.

If the Pd particle 0.2 μm in diameter were to take a core-shell structure, the value of m/k should be 0.0056, as has been discussed in Introduction. It is much smaller than the values of m/k = 0.26 - 0.29 evaluated from the oxidation titration, thermogravimetry and cyclic voltammetry. This contradiction suggests invalidity of a core-shell structure and hence supports a mixture of palladium acetate molecules and palladium atoms without localization. A loss of core-shell structure has been found for alkylcarboxyl silver nanoparticles when alkylchains became short [56].

We evaluated the diffusion coefficient of the particle by use of the

Stokes-Einstein equation, $D = k_B T/6\pi\eta r$, to be 5.6×10^{-8} cm^2 s^{-1} for the viscosity of acetonitrile, η = 0.34 mPa s. Replacing the molar concentration in Eq.(10) by the weight concentration, we can rewrite the term $(2k)c$ in Eq.(10) as

$$(2k)c = 2kc_w/ (106.4k + 224.5m) = c_w/ (53.2 + 112.2m/k) = 0.0118\ c_w \text{ (mol/g)} \quad (12)$$

where m/k = 0.28 was employed. Inserting this equation into Eq.(10), the value of $(I_p)_{A,sec}v^{-1/2}$ is 8.3 μA V$^{-1/2}$ s$^{1/2}$. The experimental slope in Figure 7 was 8.4 μA V$^{-1/2}$ s$^{1/2}$. The agreement of the experimental value with the theoretical one supports not only the diffusion-control of the particle to the electrode but also the complete oxidation without leaving any non-reacting portion. Redox latex particles larger than ca 0.1 μm diameter have exhibited partial charge transfer [18-20].The absence of the partial charge transfer in the present particle may be ascribed to a predominant component of palladium metal (75 %), which should have electric conduction inside of the particles owing to the electric percolation.

Catalytic activity

Palladium particles frequently exhibit catalytic activity [59-66]. As an example of examining the catalytic activity, we selected the reduction of methylene blue by hydrazine. 9 μM Methylene blue mixed with 4 mM hydrazine in water was kept at 20 ^oC in a given period, and the UV- and vis-spectrum was obtained, as is shown in Figure 8. The band at 664 nm is obviously due to methylene blue [59]. The absorbance decreased slowly with the time on the logarithmic scale, as is shown in Figure 9(a). When the Pd particle was added to the mixture, the spectra decreased without any deformation, indicating no influence of side reactions or light scattering of the Pd particles. The time-variation of the absorbance was much larger than that without adding the Pd particle. Therefore, the Pd particle has catalytic activity for the reduction of methylene blue with hydrazine.

The linearity of the logarithmic absorbance at 664 nm with the time indicates that

the reaction should proceed at the first-order kinetics with respect to the concentration of methylene blue. The slope of the linearity corresponds to the catalytic reaction rate constant, k. The linear variation held for several concentrations of the Pd particle c, (Figure 9(b)-(e)), at least less than 0.064 mg cm^{-3}, and hence the first-order kinetics is still valid. The reaction rate increased with an increase in c. Figure 10 shows the logarithmic variation of k with c, where k_0 is the slope in Figure 9 without Pd particles. The slope was 0.73, close to 2/3. Letting the weight of the one particle be w, the radius of the particle be r, the density be d, the number of particles added be j, the volume of the suspension be V, then we have the following equality:

$$c^{0.73} \approx \left(jw/V\right)^{2/3} = \left(j(4\pi/3)r^3 d/V\right)^{2/3} = (4\pi)^{-1/3}\left(jd/3V\right)^{2/3} 4\pi r^2 = (\text{const})S \qquad (12)$$

where S is the surface area of one particle. The catalytic reaction turns to occur on the Pd particle surface rather than as a volume reaction. The surface reaction is an essential feature of the catalysis.

The proportionality of k with S implies that the reaction zone is so small that it is regarded as the surface of the Pd particles. If the reaction zone were less than the diameter, the reaction should be observed as a volume reaction and hence the slope in Figure 10 might be unity. A catalytic reaction occurs generally only on a surface of a catalyst and hence the thickness of the reaction layer may be close to the diameter of conventional ions. Then, non-aggregated palladium ions are predicted to show a slope close to unity rather than 2/3. We carried out this catalytic reaction by use of palladium chloride. The spectra for the catalytic reaction for $PdCl_2$ were almost the same as those for the Pd particles. The reaction order was unity for $c(PdCl_2) < 0.1$ mM from the viewpoint of the proportionality of ln A at 664 nm vs. time. Figure 10 shows the plot of the rate constant against $c(PdCl_2)$ on the logarithmic scale. The slope is 0.98, indicating the shift from the surface reaction to the volume reaction.

We compare the catalytic efficiency of the Pd particles with that of $PdCl_2$. We select $\log(k - k_0 / s^{-1}) = -2.1$ as a common reaction rate constant although the slope of the

two lines are different. The corresponding concentrations (denoted as the arrows in Figure 10) are $10^{1.3}$ = 20 mg dm^{-3} for the Pd particles and $10^{-1.2}$ mM = 0.063 mM = 6.7 mg dm^{-3} for Pd^{2+} in $PdCl_2$. Since the weight ratio of palladium acetate in the Pd particle is 36 %, the effective concentration is 20×0.36 = 7.2 mg dm^{-3}. Consequently, the catalytic efficiency of the Pd particle is apparently similar to that of $PdCl_2$ per mol of salt.

Conclusion

Palladium spherical particles 0.23 μm in diameter, collected by filtration after reduction of palladium acetate, were composed of 4:1 molar ratio of palladium metal and palladium acetate. The large ratio of the palladium acetate indicates that the particles take no structure of a Pd metal core and a palladium acetate shell. The particles changed into a white bright block with heating at 400 ^{o}C. The product was like Pd bulk as if palladium powder were to be melted at much lower temperature than bulk palladium metal. The metallization by heat was of the first-order kinetics with 40 kJ mol^{-1} of the activation energy. The first order-chemical kinetics supports the significance of decomposition of the particle rather than fusion.

The colloidal suspension of the particles was electrochemically active, exhibiting the oxidation wave of Pd metal and the reduction wave of palladium acetate. The waves did not become well-defined until the purification, the centrifugation, the re-dispersion and the filtration were carried out. The currents were diffusion-controlled of the particles. The ratio of the anodic to the cathodic peak current agreed with the ratios by the partial chemical oxidation with permanganate and by the thermogravimetry. All the redox charge can be reduced and oxidized, suggesting the complete reaction. The absence of the partial charge transfer is due to keeping electric conduction inside of the particles.

The particles worked as a catalyst for the reduction of methylene blue by hydrazine. The rate constant was of the first order, and was proportional to the surface area of the Pd particles, as predicted for a surface catalytic reaction. This is in contrast with the volume catalytic reaction by palladium chloride.

References

[1] P. W. Atkins, Physical Chemistry, 6th ed., Oxford University Press, Oxford, 1998, pp.702.

[2] S. Chen, R. W. Murray, Langmuir 15 (1999) 682.

[3] L. Han, J. Luo, N. N. Kariuki, M. M. Maye, V. W. Jones, C. J. Zhong, Chem. Mater. 15 (2003) 29.

[4] E.J. Shelley, D. Ryan, S.R. Johnson, M. Couillard, D. Fitzmaurice, P.D. Nellist, Y. Chen, R.E. Palmer, J.A. Preece, Langmuir 18 (2002) 1791.

[5] A. Manna, T. Imae, T.M. Iida, N. Hisamatsu, Langmuir 17 (2001) 6000.

[6] W. Wang, X. Chen, S. Efrima, J. Phys. Chem. B 103 (1999) 7238.

[7] K. Aoki, J. Chen, N. Yang, H. Nagasawa, Langmuir 19 (2003) 9904.

[8] M.M. Maye, S. C. Chun, L. Han, D. Rabinovich, C.J. Zhong, J. Am. Chem. Soc. 124 (2002) 4958.

[9] Z. Zhong, S. Patskovskyy, P. Bouvrette, J.H.T. Luong, A. Gedanken, J. Phys. Chem. B 108 (2004) 4046.

[10] O. Tzhayik, P. Sawant, S. Efrima, E. Kovalev, J.T. Klug, Langmuir 18 (2002) 3364.

[11] A.W. Adamson, Physical Chemistry of Surfaces, 3rd ed., John Wiley & Sons, New York, 1976 p.491.

[12] H. Nagasawa, M. Maruyama, T. Komatsu, S. Isoda, T. Kobayashi, Phys. Stat. Sol. 191 (2002) 67.

[13] S. Kuwajima, Y. Okada, Y. Yoshida, K. Abe, N. Tanigaki, T. Yamaguchi, H. Nagasawa, K. Sakurai, K. Yase, Colloid. Surf. A. 197 (2002) 1.

[14] K. Abe, T. Hanada, T. Yamaguchi, H. Takiguchi, H. Nagasawa, M. Nakamoto, K. Yase, Mol. Cryst. Liq. Cryst. 322 (1998) 173.

[15] K. Abe, T. Hanada, Y. Yoshida, N. Tanigaki, H. Takiguchi, H. Nagasawa, M. Nakamoto, T. Yamaguchi, Yase, K. Thin Solid Films 327 (1998) 524.

[16] N. Yang, K. Aoki, H. Nagasawa, J. Phys. Chem. B 108 (2004) 15027.

[17] F.P. Zamborini, S.M. Gross, R.W. Murray, Langmuir 17 (2001) 481.
[18] C. Xu, K. Aoki, Langmuir 20 (2004) 10194.
[19] J. Chen, Z.J. Zhang, J. Electroanal. Chem. 583 (2005) 116.
[20] L. Han, J. Chen, I. Ikeda, Chem. Let. 342 (2005) 1512.
[21] N. Yang, K. Aoki, Electrochim Acta 50 (2005) 4868.
[22] K. Aoki, C. Wang, Langmuir 17 (2001) 7371.
[23] K. Aoki, C. Wang, J. Chen, J. Electroanal. Chem. 540 (2003) 135.
[24] K. Aoki, J. Chen, Q. Ke, S.P. Armes, D.P. Randall, Langmuir 19 (2003) 5511.
[25] P. Rijiravanich, K. Aoki, J. Chen, W. Surareungchai, M. Somasundrum, Electroanalysis 16 (2004) 605.
[26] Y. Gao, J. Chen, J. Electroanal. Chem. 578 (2005) 129.
[27] Y. Gao, J. Chen, J. Electroanal. Chem. 583 (2005) 286.
[28] S. Papp, A. Szucs, I. Dekany, Solid State Ionics 141-142 (2001) 169.
[29] W.J. Zhou, W.Z. Li, S.Q. Song, Z.H. Zhou, L.H. Jiang, G.Q. Sun, Q. Xin, K. Poulianitis, S. Kontou, P. Tsiakaras, J. Power Sources 131 (2004) 217.
[30] Y. Zhou, H. Itoh, T. Uemura, K. Naka, Y. Chujo, Langmuir 18 (2002) 277.
[31] J. Liu, L. Cheng, Y. Song, B. Liu, S. Dong, Langmuir 17 (2001**)** 6747.
[32] F.P. Zamborini, S.M. Gross, R.M. Murray, Langmuir 17 (2001) 481.
[33] Y.G. Yan, Q.X. Li, S.J. Huo, M. Ma, W.B. Cai, M. Osawa, J. Phys. Chem. B 109 (2005) 7900.
[34] D. Guo, H. Li, Electrochem. Commun. 6 (2004) 999.
[35] B. Keita, I.M. Mbomekalle, L. Nadjo, C. Haut, Electrochem. Commun. 6 (2004) 978.
[36] M. Platt, R.A.W. Dryfe, E.P.L. Roberts, Electrochim. Acta 49 (2004) 3937.
[37] M. Yamada, H. Nishihara, C. R. Chimie 6 (2003) 919.
[38] M.M. Alvarez, J.T. Khoury, T.G. Schaaff, M.N. Shafigullin, I. Verzmar, R.L. Whetten, J. Phys. Chem. B 101 (1997) 3706.
[39] S.W. Chen, K. Huang, J.A. Stearns, Chem. Mater. 12 (2000) 540.
[40] T. Teranishi, M. Miyake, Chem. Mater. 10 (1998) 594.
[41] S.W. Chen, R.W. Murray, S.W. Feldberg, J. Phys. Chem. B 102 (1998) 9898.
[42] D.J. Guo, H.L. Li, Electrochem. Comm. 6 (2004) 999.
[43] P.Z. Pawlow, Phys. Chem. 65 (1909) 545.
[44] H. Reiss, I.B. Wilson, J. Colloid. Sci. 3 (1948) 551.
[45] J.-P. Borel, Surf. Sci. 106 (1981) 1.
[46] J. Ross, R.P. Andress, Surf. Sci. 106 (1981) 11.

[47] Y. Shimizu, S. Sawada, K.S. Ikeda, Eur. Phys. J. D. 4 (1998) 365.
[48] K.F. Peters, J.B. Cohen, Y.-W. Chung, Phys. Rev. B 57 (1998) 13430.
[49] H.W. Sheng, K. Lu, E. Ma, Nanostruct. Mater. 10 (1998) 865.
[50] C.L. Cleveland, W.D. Luedtke, U. Landman, Phys. Rev. B 60 (1999) 5065.
[51] R. Kofman, P. Cheyssac, A. Aouaj, Y. Lereah, G. Deutscher, T. B-David, J.M. Penisson, A. Bourret, Surf. Sci. 303 (1994) 231.
[52] H. Sakai, Surf. Sci. 348 (1996) 387.
[53] T.L. Beck, J. Jellinek, R.S. Berry, J. Chem. Phys. 87 (1987) 545.
[54] J.D. Honeycutt, H.C. Andreson, J. Phys. Chem. 91 (1987) 4950.
[55] A.W. Adamson, Physical Chemistry of Surfaces, 3rd ed., John Wiley & Sons, New York, 1976 p. 334.
[56] N.Yang, K. Aoki, J. Phys. Chem. B 109 (2005) 23911.
[57] A.J. Bard, L.R. Faulkner, Electrochemical Methods, Fundamentals and Applications, 2nd ed., John Wiley & Sons, New York, 2001, p.231.
[58] K. Aoki, Electroanalysis 17 (2005) 1379.
[59] N.R. Jana, Z.L. Wang, T. Pal, Langmuir 16 (2000) 2457.
[60] N.R. Jana, T. Pal, Langmuir 15 (1999) 3458.
[61] R. Gomez, J.M. Perez, J. Solla-Gullon, V. Montiel, A. Aldaz, J. Phys. Chem. B 108 (2004) 9943.
[62] J. Solla-Gullon, A. Rodes, V. Montiel, A. Aldaz, J. Clavilier, J. Electroanal. Chem. 554 /555 (2003) 273.
[63] Y. Lin, X. Cui, X. Ye, Electrochem. Commun. 7 (2005) 267.
[64] Y.-F. Han, D. Kumar, D.W. Goodman, J. Catal. 230 (2005) 353.
[65] J.E. Park, S.G. Park, A. Koukitu, O. Hatozaki, N. Oyama, Synthetic Met. 141 (2004) 265.
[66] J. Solla-Gullon, V. Montiel, A. Aldaz, J. Clavilier, Electrochem. Commun. 4 (2002) 716.

Figure Captions

Figure 1. Spectra of (a) 0.05 mM $Pd(COO(CH_3))_2$ and (b) 0.01 mg cm^{-3} Pd particles in dichloromethane.

Figure 2. SEM photograph of the Pd particles (A) before and (B) after the centrifugation and the filtration through 0.2 μm micropore filter. (C) displays the size distribution (number of the particles vs. radii) of the filtered particles.

Figure 3. Thermogravimetric curve at scan rate, 10 $^oC\ min^{-1}$.

Figure 4. Analysis of thermogravimetric curve in Figure 3 by use of the first-order decomposition reaction. The slope of the line corresponds to $-U/R$.

Figure 5. Cyclic voltammograms with waves (a) and (b) of 0.55 mg cm^{-3} Pd particles in acetonitrile including 0.05 M $TBAPF_6$ at v = 0.15 V s^{-1} at the Pt electrode. Wave (c) is for the blank solution at v = 0.15 V s^{-1} at the Pt electrode. Voltammogram (d) is at the palladium electrode in acetonitrile including 0.05 M $TBAPF_6$ at v = 0.15 V s^{-1}.

Figure 6. Variations of the anodic and the cathodic peak current with the concentration of Pd particles at v = 0.1 V s^{-1} at the Pt electrode.

Figure 7. Dependence of the anodic and the cathodic peak current on the square-root of the scan rate in the solution of 0.55 mg cm^{-3} Pd particles at the Pt electrode.

Figure 8. Time-variation of UV spectra of the solution of 9 μM methylene blue and 4 mM hydrazine (a) 0, (b) 1, (c) 2 and (d) 3 min after the addition of 0.02 mg cm^{-3} Pd particles.

Figure 9. Time-variation of the absorbance at 664 nm of the mixture of 9 μM methylene blue and 4 mM hydrazine after addition of (a) 0, (b) 8, (c) 18, (d) 56, and (e) 64 mg dm^{-3} Pd particles.

Figure10 Logarithmic dependence of the first-order rate constants on concentration of Pd particles on the lower x-axis and $PdCl_2$ on the upper x-axis. The rate constants were obtained from the slopes in Figure 9.

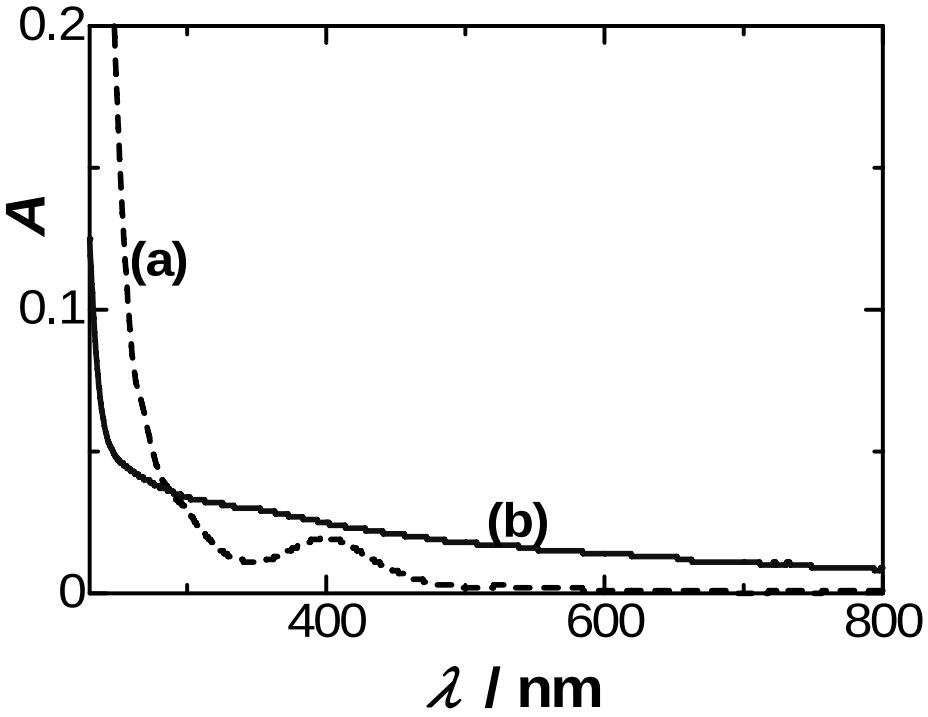

Figure 1

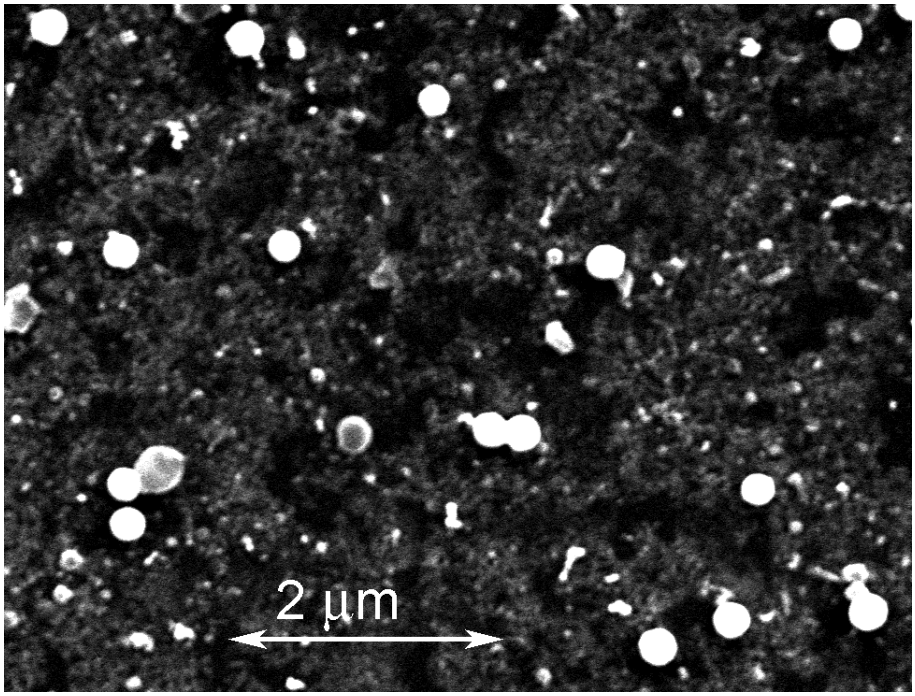

Figure 2(A)

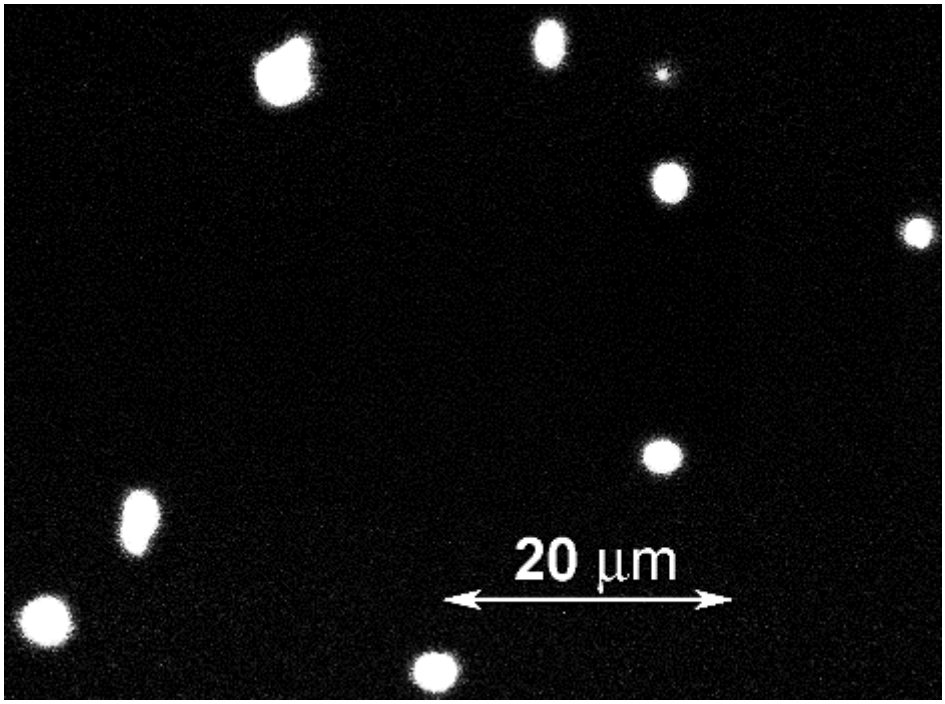

Figure 2(B)

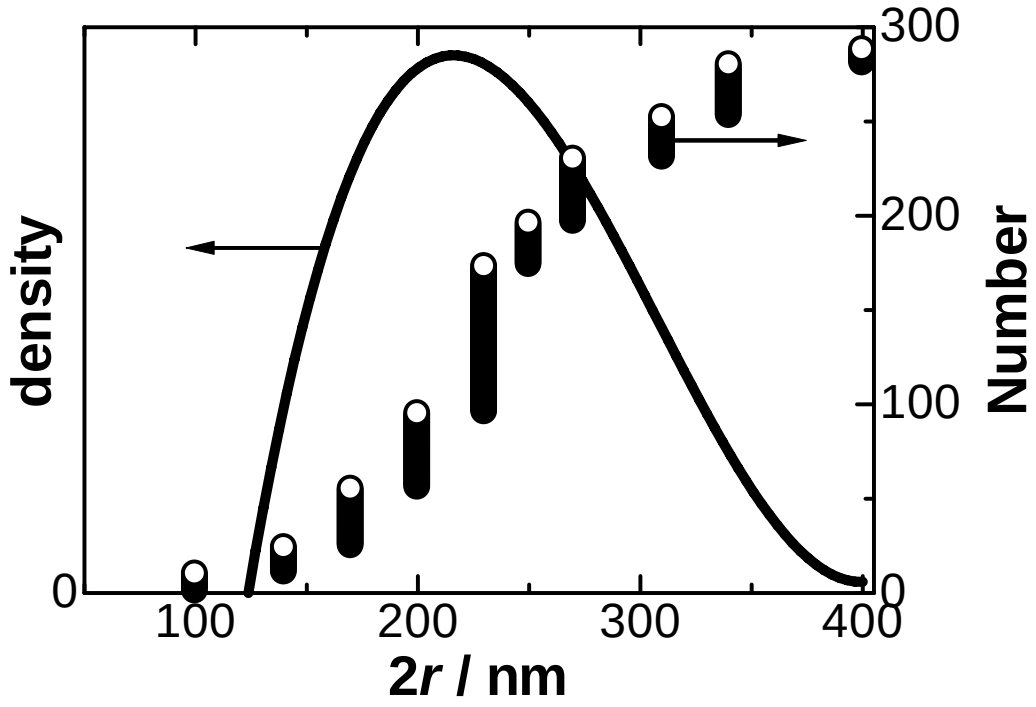

Figure 2(C)

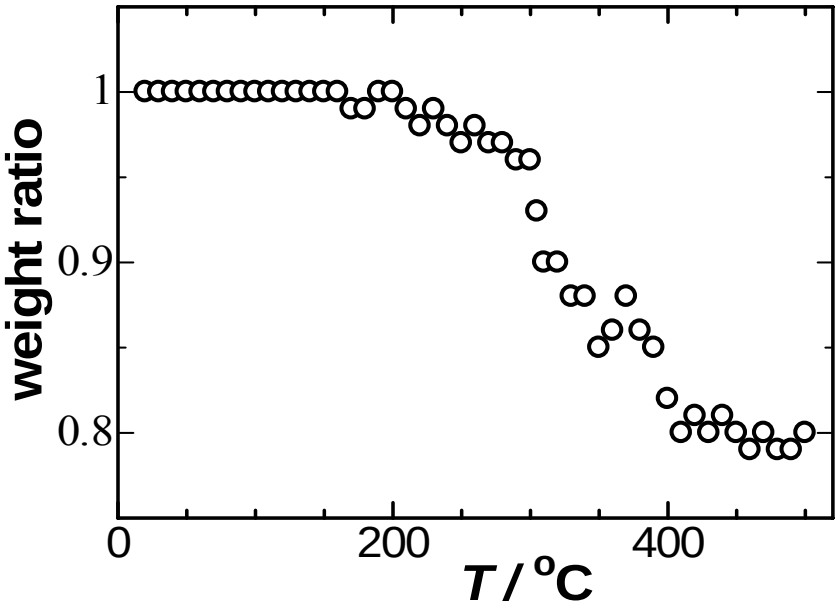

Figure 3

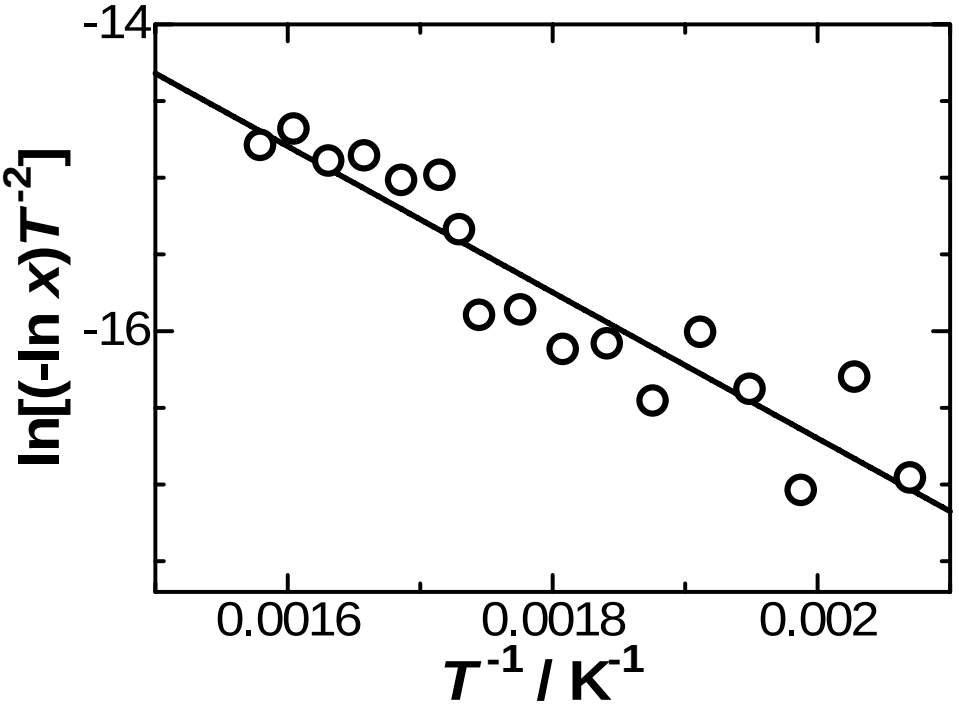

Figure 4

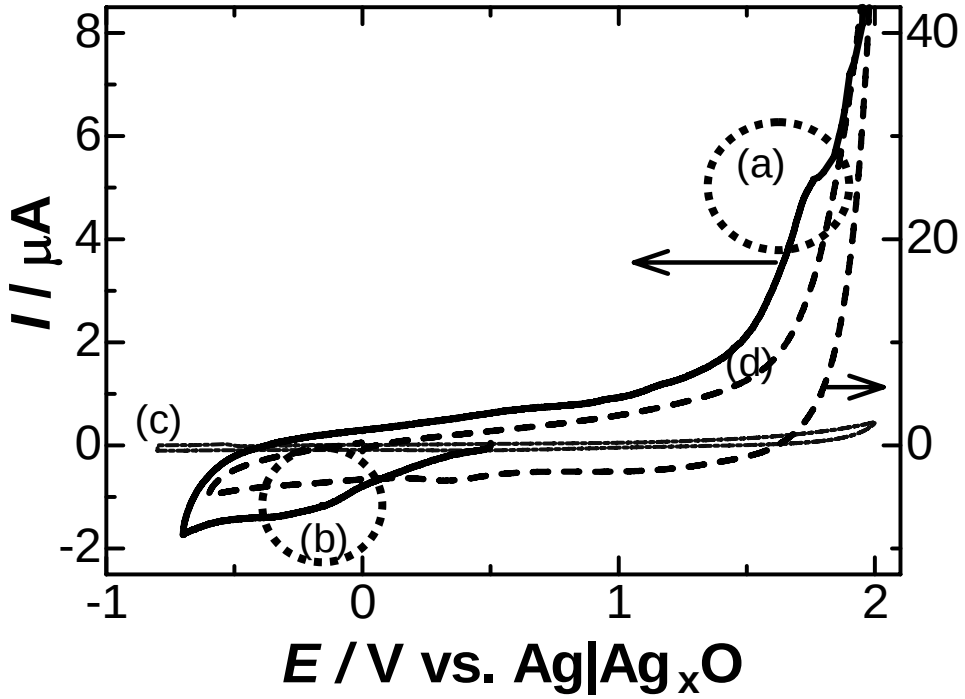

Figure 5

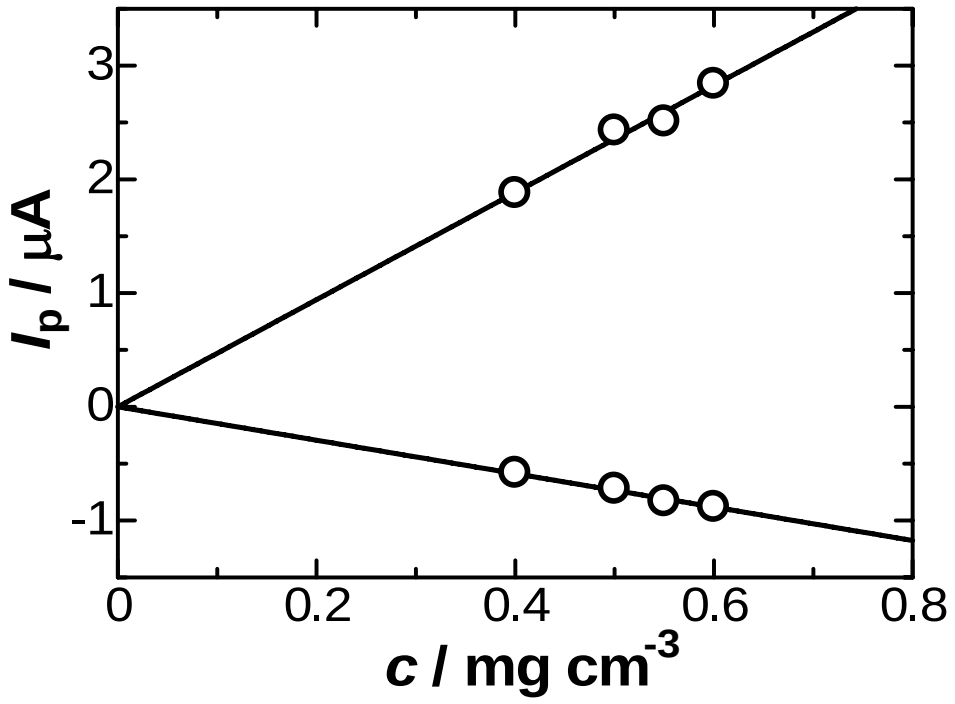

Figure 6

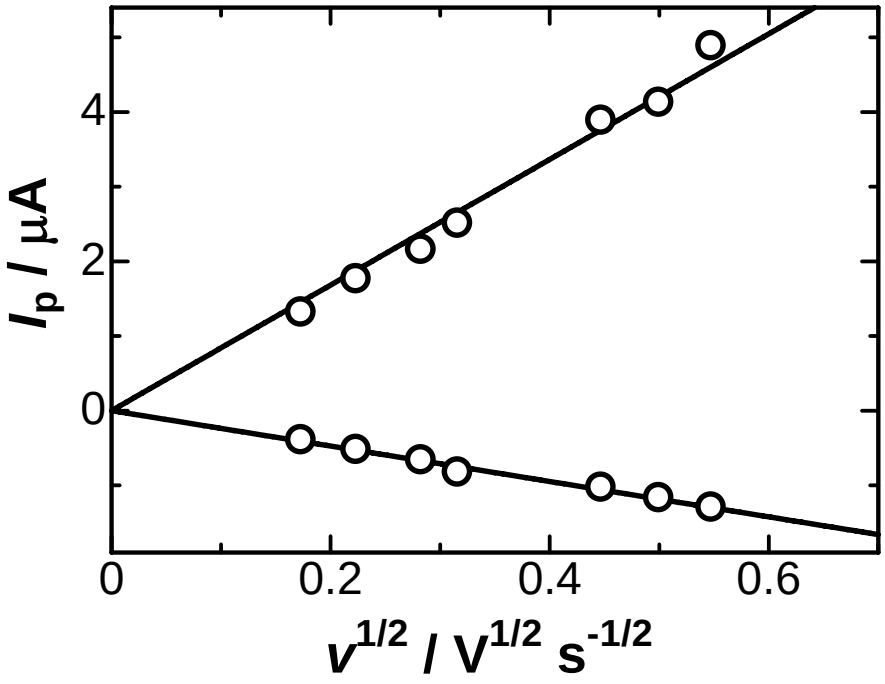

Figure 7

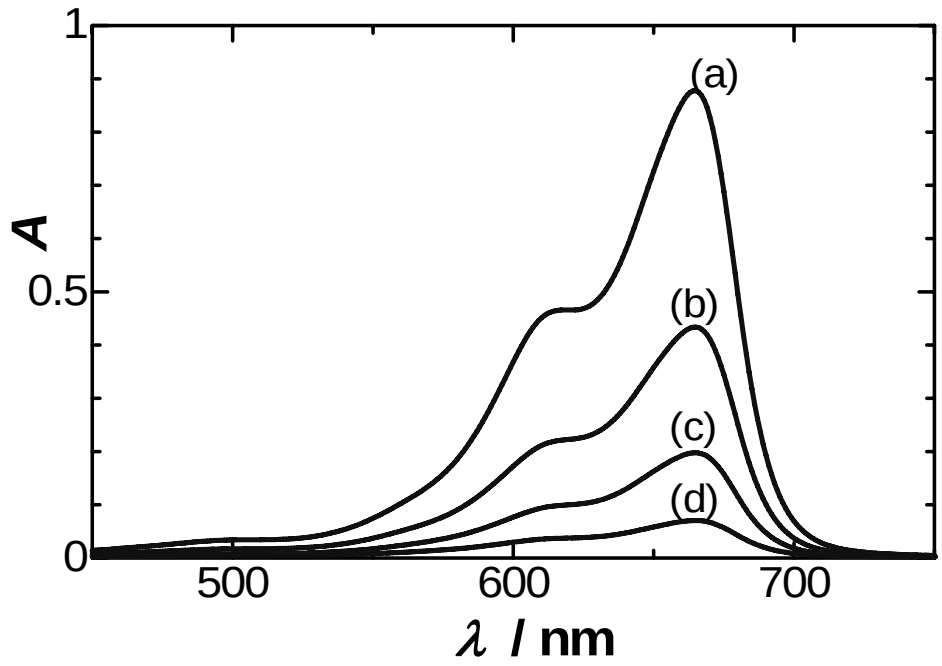

Figure 8

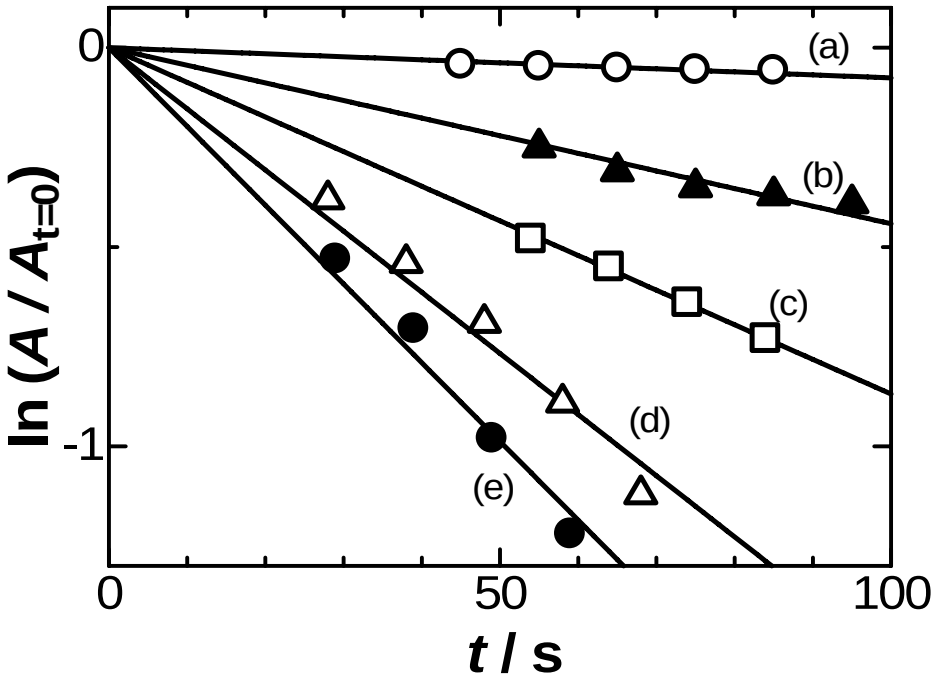

Figure 9

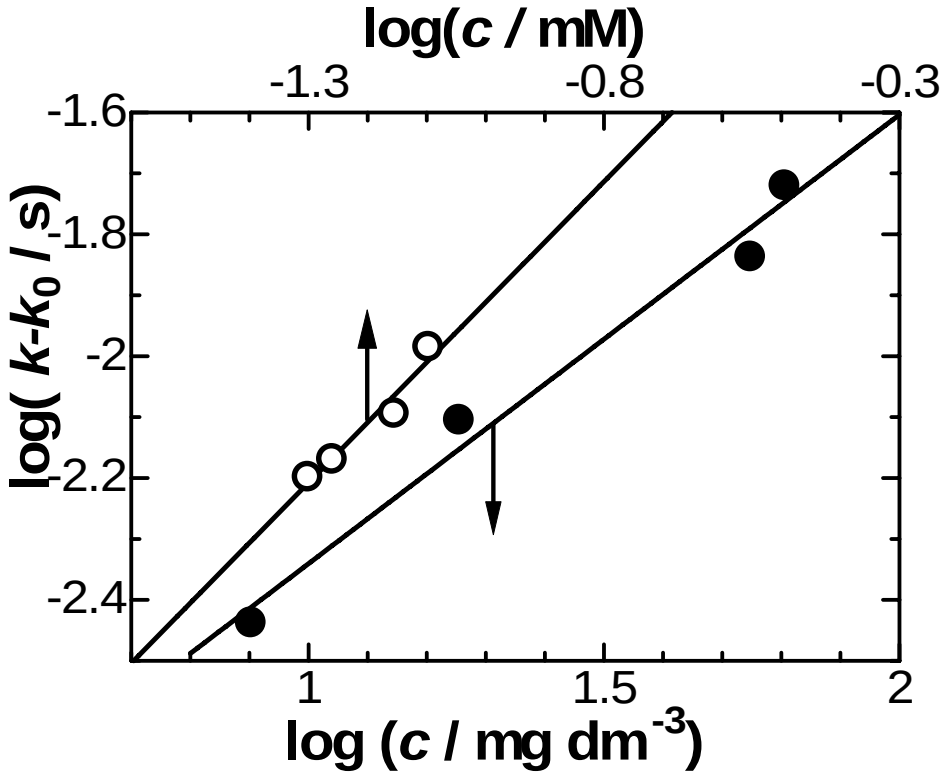

Figure 10

Table 1. Combination of Eq.(9) and (10)

	$(I_p)_C/(I_p)_A$		m / k			
	A,com	A,sec	A,com		A,sec	
			I_p vs. c	I_p vs. $v^{1/2}$	I_p vs. c	I_p vs. $v^{1/2}$
C,com	m / k	$m / 2^{1/2}k$	0.31	0.28*	0.44	0.40
C,sec	$2^{1/2}m / k$	m / k	0.22	0.20	0.31	0.28*